

The physics of karate

S. R. Wilk,^{a)} R. E. McNair,^{b)} and M.S. Feld

Department of Physics and Spectroscopy Laboratory, Massachusetts Institute of Technology, Cambridge, Massachusetts 02139

(Received 20 July 1982; accepted for publication 28 September 1982)

This study analyzes physical aspects of a karate strike and its interaction with a target, examining some heretofore unexplored dynamical and biomechanical questions.

I. INTRODUCTION

In recent years, the martial arts has experienced a revitalization and achieved worldwide popularity. It is extraordinary that as early as 2000 years ago ancient Oriental priests, warriors, and physicians devised systems of weaponless self-defense that make nearly optimal use of the human body. Many of the stances and techniques employed are totally different from the combat methods of the Western world and are often counterintuitive. The ways in which animal movements were studied and incorporated into exercise forms, and the gradual infusion of militaristic and religious doctrines which led to karate, tae kwon do, tai chi, and other Asian fighting arts are well documented.¹

Karate itself developed in Okinawa in the early 17th century when the Japanese conquered the island and confiscated all weapons. In order to continue their feudal practices, the Okinawans developed a system of combat based on the weaponless Chinese fighting methods. The Japanese word karate means Chinese hand or empty hand. Today these ancient techniques, along with the associated rituals and mental discipline, are practiced throughout the world. Though some variations have been introduced in modern styles and methods, the fundamentals of karate techniques remain unaltered and the development of these techniques follows the same general scenario as in the ancient systems.

The perfection of basic techniques is the prime objective of the karateka, the practitioner of the martial arts. To this end, the repetition of a variety of striking, kicking, and blocking techniques is the major constituent of a karate training session, with emphasis placed on proper breathing, balance, and focus. The development of these skills is further enhanced through the study of the "kata," each one a series of prescribed blocks and counterattacks against a number of imaginary attackers, and through free-style sparring (kumite), wherein the elements of timing and mental conditioning are incorporated.

The renewed interest in the martial arts has been stimulated, in part, by demonstrations in which martial arts practitioners perform physical and mental feats which often defy one's reasoning and intuition, thereby leaving an observer in awe. The destruction of formidable piles of wood and concrete by bare hands, feet, or other parts of the body (Fig. 1) is a dramatic manifestation of the inherent destructive capability of the human body. Although the breaking of objects is often the most memorable and sensational aspect of a karate demonstration, it is *not* an inherent part of karate. Breaking is neither an objective of the karateka nor an item in regular training; it is used primarily to gauge and demonstrate the effectiveness of various techniques. It is in this spirit that this article studies breaking as a measure of the effectiveness of the martial arts as a means of self-defense.

Recently, the underlying physical principles of the mar-

tial arts have begun to be explored through the study of karate strikes and the breaking of objects. Walker² has examined kinematical aspects of a karate punch, and he and Blum³ have analyzed the breaking process, treating the interaction of hand and block in the static approximation. Cavanaugh and Landa,⁴ Vos and Binkhorst,⁵ and Tuinzing and Fischera⁶ have measured different aspects of karate strikes through the use of force plates, stroboscopy, accelerometry, and electromiography. The present study further analyzes physical aspects of a karate strike and its interaction with a target, examining some heretofore unexplored dynamical and biomechanical questions.

An analysis of the deflection and subsequent fracture of a slab of material leads to expressions for the stored internal energy, time, and force required for breaking in terms of the bulk properties of the target. These quantities are measured by means of static loading, force plate, and acoustical techniques. Trajectories, velocities, and peak energies of karate techniques are also studied using two- and three-dimensional stroboscopic techniques. High-speed movies of the impact of the striking part of the body with the target are used to obtain detailed information about the deceleration and deformation of the fist during the strike, and hence the forces acting on it, and the onset of fracture in the target. The transfer of the kinetic energy of a strike into elastic energy in the target is explored both by simple mechanical approximations and a more quantitative dynamic model. The latter gives good agreement with the data and provides insight into the forces acting in the hand-forearm system. The ways in which the striking part of the body, properly positioned, protects itself from damage are also discussed.

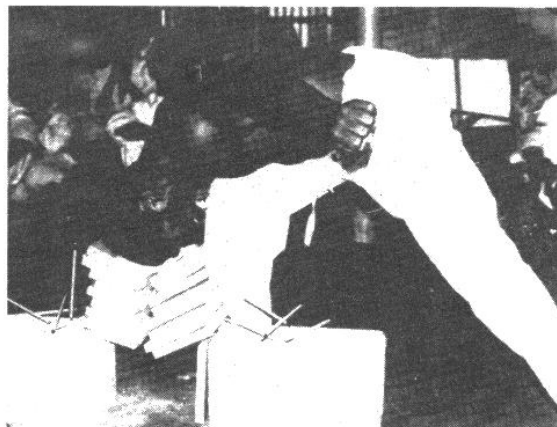


Fig. 1. Fracture of a stack of wooden boards using the forehead.

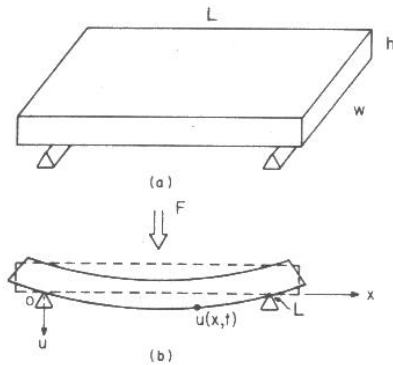


Fig. 2. Dimensions of blocks and their coordinates.

II. DYNAMICAL THEORY OF BREAKING

The blocks used in this study are rectangular bars of wood and concrete. Their dimensions l , w , h , and coordinates are defined in Fig. 2. x is the position along the length l . $u(x,t)$ is the deflection of the bottom surface from its equilibrium position.

The concrete bars are "patio blocks" made of type III cement and measuring $lwh = 40 \times 19 \times 4.0$ cm. The wooden blocks are pieces of dry white pine 1×12 -in. shelving board measuring $28 \times 15 \times 1.9$ cm, cut so that the grain runs parallel to the width w . The patio blocks are dried in an oven for several hours to remove excess water, and thus improve the uniformity of the samples. In either case the blocks are supported at each end of their longest dimension, l , with their shortest dimension, h , vertical (Fig. 2). Two centimeters of overhang are allowed for at each end, reducing the effective length of the blocks by 4 cm. The mass of the blocks is 6.5 and 0.28 kg for concrete and wood, respectively.

The block is struck by the karateka at the top surface near the center of the span. For simplicity the force exerted by the striker is assumed to be evenly distributed along the line $x = l/2$, thus eliminating from consideration variations along w and reducing the problem to two dimensions. It is further assumed (and experiment confirms) that the deflection of the block is small compared to its overall dimensions.

Under these conditions the deflection $u(x,t)$ of a bar of density ρ and cross-sectional area $A = hw$ to an applied force is given, to good approximation, by the equation⁷

$$\rho A \frac{\partial^2 u}{\partial t^2} + EI \frac{\partial^4 u}{\partial x^4} = \mathcal{F}(x,t), \quad (1)$$

where \mathcal{F} is the force per unit length exerted on the bar and E is the Young's modulus of elasticity of the material. I , the moment of inertia for the cross section of the bar, depends only on its shape and dimensions. For a rectangular bar

$$I = h^3 w / 12. \quad (2)$$

For the case of free vibrations ($\mathcal{F} = 0$) solutions to Eq. (1) are of the form

$$u(x,t) = C \sin\left(\frac{n\pi x}{l}\right) \sin \omega_n t, \\ \omega_n = \left(\frac{n\pi}{l}\right)^2 \left(\frac{EI}{\rho A}\right)^{1/2}, \quad n = 1, 2, \dots \quad (3)$$

If the impact occurs over a time interval $\gg 2\pi/\omega_2$ only

the lowest mode ($n = 1$) will be appreciably excited, and the deflection is of the form

$$u(x,t) = \sin(\pi x/l) d(t), \quad (4)$$

with d the time-dependent part of u . Equation (1) can then be reduced to a simple form by substituting Eq. (4), multiplying both sides by $\sin(\pi x/l)$, and integrating over x from 0 to l . Since the force is applied at $x = l/2$ the right-hand side of Eq. (1) is of the form $\mathcal{F}(x,t) = F(t)\delta(x - l/2)$. This yields

$$\ddot{d} + \omega^2 d = (2/\rho A l) F(t). \quad (5)$$

Thus the motion of the block reduces to that of a harmonic oscillator of mass

$$m = \rho A l / 2 \quad (6a)$$

and spring constant

$$k = m\omega^2 = \frac{\pi^4 EI}{2l^3} = \frac{\pi^4}{24} \frac{h^3 w}{l^3} E. \quad (6b)$$

The downward deflection of the block gives rise to stresses within it, the largest component, σ_x , being directed along l (x axis). This produces an elongation⁸ along x , hence a strain, ϵ . The block fractures when, at some point x , σ reaches a critical value, σ_0 , called the modulus of rupture. If the stresses along w and h are small compared to σ then the simple Hooke's law relation $\sigma = \epsilon E$ holds.⁹ Using the well-known relationship between ϵ and u ,¹⁰

$$\sigma = \epsilon E = Ey \frac{\partial^2 u}{\partial x^2}, \quad (7)$$

where y is the distance of a point inside the block to the plane which bisects the block horizontally. Inserting Eq. (4) gives

$$\sigma = -(\pi/l)^2 Ey \sin(\pi x/l) d(t). \quad (8)$$

The greatest stress occurs at $x = l/2$ and $y = \pm h/2$. Thus the fracture begins at the center of the surface of the block and rapidly propagates inward. In practice, the crack begins at the lower surface, since materials such as wood and concrete are stronger under compression than in stretching.^{8,11}

The value of d at which fracture occurs may be obtained from Eq. (6):

$$d_0 = \frac{2l^2 \sigma_0}{\pi^2 h E}. \quad (9)$$

Using the value of the spring constant obtained in Eq. (6b), one can obtain expressions for the stored energy U_0 and the force F_0 exerted by the block at the point of fracture:

$$U_0 = \frac{1}{2} k d_0^2 = (\sigma_0^2 / 12E) h w l, \quad (10)$$

$$F_0 = k d_0 = (\pi^2 / 12) (h^2 w / l) \sigma_0. \quad (11)$$

These results are similar to those of Walker² and Blum,³ obtained by assuming that the shape of the dynamically deformed block is the same as for static loading.¹²

In order to evaluate U_0 and F_0 , values for the modulus of rupture and elasticity for our wood and concrete samples are needed. We have found it necessary to measure these parameters ourselves. In the case of concrete E and σ_0 vary considerably due to water content, age, and type of material.^{11,13} As for wood, although tabulated values of the modulus for several different types are available (as in the USDA *Woods Handbook*), it appears that the parameters are measured for the wood stressed along the direction of the grain. They are therefore not applicable to our samples.

Table I. Breaking parameters for wood, concrete, and bone.

	Wood	Concrete	Bone
$E(10^8 \text{ N/m}^2)$	1.4 ± 0.5	28 ± 9	180^a
$\sigma_0(10^6 \text{ N/m}^2)$	3.6 ± 1.0	4.5 ± 0.5	210^a
$d_0(\text{mm})$	16 ± 7	1.1 ± 0.4	11^b
$U_0(\text{J})$	5.3 ± 2.8	1.6 ± 0.6	14^b
$F_0(10^2 \text{ N})$	6.7 ± 1.9	31 ± 3.5	54^b

^aRepresentative values from Yadama, Ref. 15.

^bAssumes a cylindrical bar of length 30 cm and radius 1 cm.¹⁵

The values of E and σ_0 were thus determined experimentally. A hydraulic testing machine was used to deflect the center of simply supported blocks identical to those used in the breaking studies. Graphs of the applied force f versus the peak deflection δ were made from which the moduli were determined making use of formulas of the type¹⁴

$$\sigma_0 = \frac{3}{2}(l/h^2w)f, \quad (12a)$$

$$E = (l^3/48I\delta)f. \quad (12b)$$

The results are shown in Table I, along with the resulting values of d_0 , U_0 , and F_0 .¹⁵ For concrete our values for the moduli agree with the tabulated ones,^{11,13} but for wood our values are considerably smaller.¹⁶ For comparison the corresponding values for a long bone¹⁷ are also given. As can be seen, the force needed to rupture such a bone is much greater than in the case of either wood or concrete, primarily because of the correspondingly larger value of σ_0 .

As a check, the acoustical vibrations induced by lightly tapping the simply supported slabs with a pencil eraser were monitored by means of a small microphone. For the concrete blocks the lowest mode could be excited easily, yielding oscillations of period ≈ 5 ms which decayed in about 60 ms (Fig. 3). This is in reasonable agreement with the period of $6.6 \text{ ms} \pm 20\%$ predicted by Eq. (3). For the wood blocks a complex aperiodic acoustical pattern of peaks was observed, the largest ones being separated by 7–8 ms, as compared with the predicted value of $11 \text{ ms} \pm 20\%$. The nonsinusoidal behavior indicates that tapping unavoidably excites many modes, possibly including those when the slab responds as a plate rather than a bar,⁷ and probably

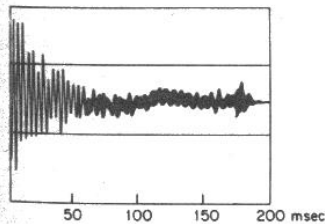
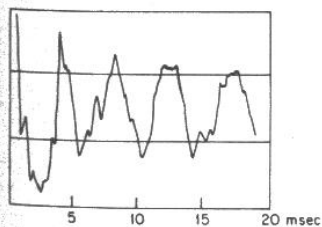


Fig. 3. Acoustical vibrations of a concrete slab, simply supported as in Fig. 2.



reflects the highly anisotropic elastic character of wood. The approximations made in the treatment above are better satisfied under karate strike excitation, where the duration of the impact is much longer so that the higher order modes are damped out during the interaction.

III. KINEMATICAL STUDIES OF KARATE TECHNIQUES

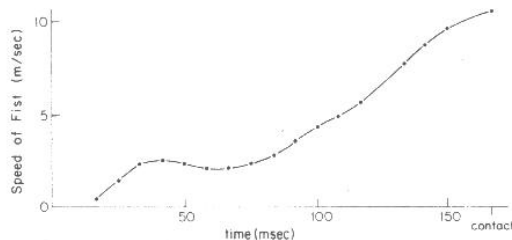
Since only a portion of the initial energy of the part of the body delivering the blow can be imparted to the target, the striker must have considerably more energy than U_0 if the block is to fracture. In order to determine the velocities, accelerations, etc. and the energies available to various techniques, strobe photographs were taken with an EEG model 553-11 Multiflash strobe lamp at 60 or 120 flashes/s. A variety of approaches was used: single exposures, acoustically triggered by the initial impact; multiple exposures; and sequential exposures using a rotating drum camera. In cases in which the motion was not in a plane, front and side views were recorded simultaneously by means of a large mirror placed to one side of the subject at 45° to the line of sight. The three-dimensional trajectory was then reconstructed using computer analysis,¹⁸ from which peak velocities and other kinematical parameters could be determined.

As an example of the latter approach, Fig. 4(a) shows one frame of a drum camera sequence of a hammerfist strike (kensui-uchi), giving front and side views simultaneously. From this sequence the net speed of the hand as a function of time could be determined [Fig. 4(b)]. In this case a peak velocity of 10 m/s was reached at the point of impact. Other sequences with the same subject gave values as high as 14 m/s.

The results of the strobe studies are summarized in Table II. Peak speeds of 10–14 m/s were measured for hammer-



(a)



(b)

Fig. 4. Strobe photo analysis of hammerfist strike. (a) Single frame of drum camera sequence showing side and front views simultaneously. (b) Net speed of fist versus time, obtained from sequence.

Table II. Maximum speeds attained in various karate techniques, as measured from strobe photo studies of various subjects.

Technique	Maximum speed (m/s)
Front forward punch (seikan zuki)	5.7-9.8
Downward hammerfist strike (kentsui-uchi)	10-14
Downward knife hand strike (shuto-uchi)	10-14
Wheel kick	7.3-10
Roundhouse kick (mawashi-geri)	9.5-11
Back kick (ushiro-geri)	10.6-12
Front kick (mae-geri)	9.9-14.4
Side kick (yoko-geri)	9.9-14.4

fist and knife hand strikes (shuto-uchi), while somewhat smaller values were obtained for strikes in which the striking surface was the heel of the hand (shote-uchi). By way of comparison, forward punches (seikan-zuki) were found to reach speeds of 5.7-9.8 m/s, and various kicks 7.3-14.4 m/s.

Defensive techniques were also studied stroboscopically. Figure 5 shows a multiple strobe exposure of a downward block (gedan-barai), used to deflect an incoming blow to the lower portion of the body. As can be seen from the photo, maximum velocity is reached as the fist moves past the solar plexus region, well before the point of contact. This is different from offensive techniques, such as the hammerfist of Fig. 4 and the forward punch of Fig. 2 in Ref. 2, in which the peak velocity is reached at the point of contact. This feature is characteristic of blocks, whose purpose is to redirect an incoming technique and render it harmless rather than to meet it directly, a function which does not require developing large amounts of momentum.

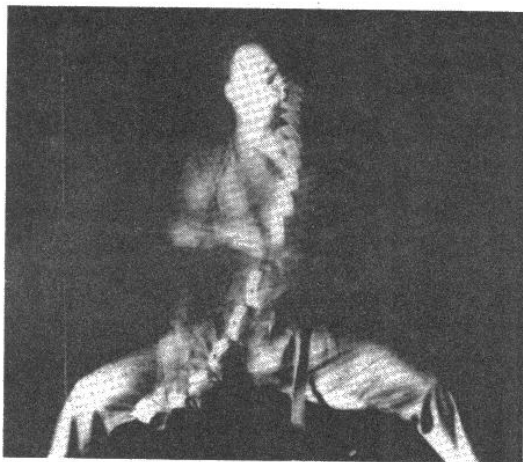


Fig. 5. Multiple strobe exposure of a downward block, 120 flashes/s.

The fist velocities measured in this study are comparable to those reported previously by other researchers. Vos and Binkhorst⁵ measured velocities of 10-14 m/s in downward strikes, and Cavanaugh and Landa⁴ reported angular velocities at the elbow of 24-29 rad/s. These agree with our measurements, 6-14 m/s and 25-27 rad/s, respectively. The time evolution of the forward punch recorded by Walker² is similar in shape and magnitude to those we measured.

IV. DETAILS OF THE IMPACT PROCESS

For a more detailed look at the collision between striker and target high-speed movies (1000 and 5000 frames/s) were taken. Figure 6 shows a sequence of frames of a hammerfist strike impinging on a concrete block. Successive frames are separated in time by 1 ms. These photos show the rapid deceleration of the fist on contact and its compression, and the subsequent initiation of the crack at the lower surface of the block and its rapid propagation upwards.

In analyzing such film strips the positions of the four marker dots on the fist were carefully recorded over a series of frames. The velocity and acceleration of each dot was then obtained by numerical differentiation. The results for the strike of Fig. 6 are shown in Fig. 7, in which is plotted the vertical position of the lower right dot and the corresponding velocity and acceleration. As the fist strikes the block it undergoes an extremely rapid deceleration, reaching a maximum value of 3500 m/s² for the lower right dot (Fig. 7) and up to 4000 m/s² for the other three. This brings the fist to a standstill, after which it continues downward. As seen in Fig. 7, the interaction lasts for 5 ms.

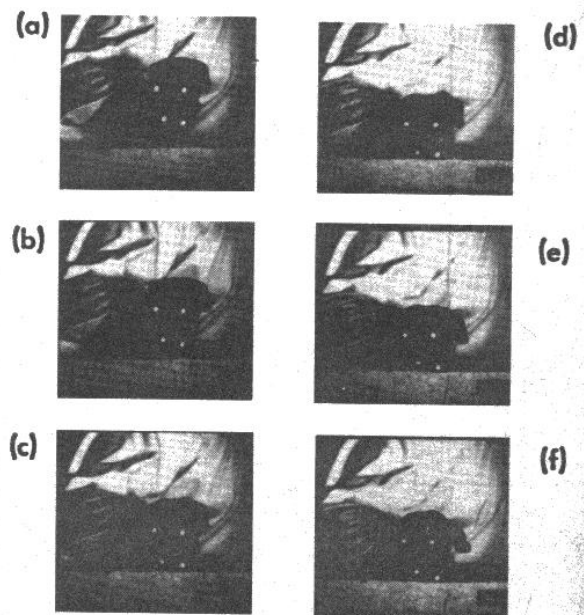


Fig. 6. Hammerfist strike impinging on a concrete patio block, high-speed movie film. Time between frames is 1 ms. The four dots are markers used as reference points. Although contact is made in frame (c), the crack does not develop until frame (e). Fracture occurs when the crack reaches the upper surface. Elapsed times for these frames are (a) 0, (b) 1, (c) 2, (d) 3, (e) 4, and (f) 5 ms.

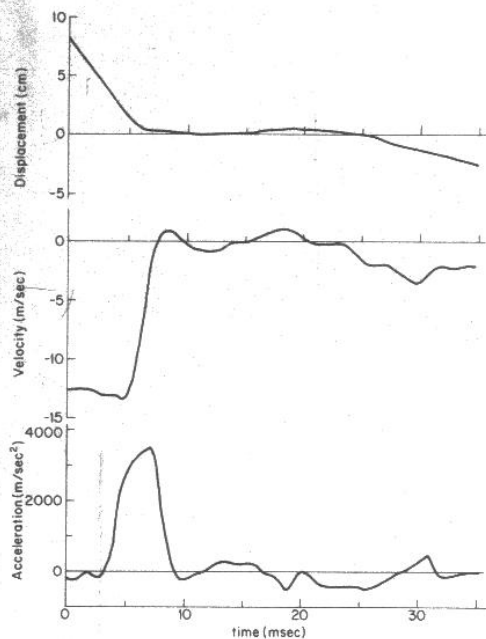


Fig. 7. Position, velocity, and acceleration of lower right-hand dot of fist from filmstrip of Fig. 6.

This data may be used to estimate the peak force exerted on the fist during impact, given by the product of the hand mass and its acceleration. Applying the predictive formulas for the mass of body parts developed by Clauser *et al.*¹⁹ to our subjects, we obtained an estimate of 0.7 kg for the mass of the fist. This yields peak forces in the range of 2400–2800 N.

Similar high-speed movies were also made using wood blocks, but decelerations when the fist strikes wood are very small and hard to measure.

Finally, as a check of the forces required to fracture the samples under actual conditions several blocks, supported at their ends on cinder blocks atop a force plate, were broken by karate strikes. The setup is essentially the same as that used by Vos and Binkhorst.⁵ The force plate measures the force of the block pressing against the supports, hence the reaction force of the block (i.e., the product of its effective spring constant and displacement). The time dependence of the output signals, displayed on an oscilloscope, was about the same for both wood and concrete: The force rises rapidly over a period of 3–5 ms, after which the block either breaks or rebounds. For concrete, peak values as large as 2900 N were recorded when fracture occurred, with a mean peak value of 1900 N. The corresponding mean value for wood was 600 N. These are in reasonable agreement with the corresponding values of Table I. Interestingly enough, larger values were recorded when fracture did not occur, as large as 3600 N for concrete. Vos and Binkhorst⁵ also observed larger peak values for unsuccessful breaks. This indicates (i) that the subject was capable of generating more than the required force for fracture, and (ii) that the force exerted by the striker is not the only important parameter—proper positioning of the hand or foot and its contact point along the length of the block are also critical.

The importance of making contact at the center of the target is graphically illustrated in the strobe photos of Fig.



Fig. 8. Incomplete breaks of stacks of (a) wood and (b) concrete blocks. The technique in (a) is a hammerfist strike, and in (b) a palm-heel (shote) thrust.

8, which show incomplete breaks of stacks of (a) wood and (b) concrete blocks, separated by means of pencils at the ends. In each case all of the blocks were broken except for the bottom one, which remained intact. The subjects were capable of breaking the entire stack when the target was struck at the center, and failure to do so was attributed to the fact, evident in the photos, that contact occurred to the side of the target. This conclusion is further supported by the fracture pattern formed in successive blocks, which depicts the shock wave propagating towards the center of the stack. Photos such as these also reveal that the blocks fracture in succession, and that direct contact with the hand is not needed. This is particularly apparent in Fig. 8(a), where nine boards have been broken although the fist has only moved past the top two. Thus as a given block undergoes fracture it develops sufficient linear and angular momentum to fracture the block beneath it which, in turn, can fracture the next block. Huge stacks of material can be broken in this way.

V. COUPLING OF ENERGY INTO A TARGET

We seek a model that accounts for the behavior of the block and the hand during impact. As a specific example,

Table III(a). Initial velocities v_i and kinetic energies U_i needed to fracture slab. The uncertainties are due to variations among samples.

		Elastic		Collision model Inelastic		Dynamic ²⁰	
		v_i (m/s)	U_i (J)	v_i (m/s)	U_i (J)	v_i (m/s)	U_i (J)
Slab material	Wood	5.2 ± 1.9	9.5 ± 5.0	4.3 ± 1.6	6.4 ± 3.4	6.1	12.3
	Concrete	2.8 ± 0.85	2.7 ± 1.0	5.0 ± 1.5	8.9 ± 3.3	10.6	37.1

the following discussion considers a downward hammerfist strike. In this technique the hand is tightly clenched and the block is struck with the bottom surface of the fist [Fig. 4(a)]. Consider first the rough approximation in which the interaction is assumed to be a simple mechanical collision—either elastic or inelastic. This approach necessitates choosing a value for the effective mass M of the hand-forearm system. High-speed films taken in side view indicate that in this technique the fist pivots at the wrist during impact, and that the resulting shock wave does not reach most of the forearm until after the block has fractured. Thus the appropriate value for M is the fist mass, ~ 0.7 kg.

The minimum initial kinetic energy, U_i , the hand must have in order to impart U_0 to the block is given by

$$\text{inelastic collision: } U_i = [(m + M)/M]U_0 \quad (13a)$$

(energy imparted to block-hand system),

$$\text{elastic collision: } U_i = [(m + M)^2/4mM]U_0. \quad (13b)$$

The effective mass m is 0.14 kg for wood and 3.2 kg for concrete [Eq. (6a)]. The resulting initial energies and velocities are given in Table III. The inelastic predictions for U_i of 6.4 and 8.9 J for wood and concrete, respectively, appear to be reasonable (although perhaps too small), but the corresponding elastic values of 9.5 and 2.7 J do not, as they predict that the concrete targets are much easier to break than the wooden ones, in clear contradiction to experience. For the same reason both elastic and inelastic predictions using a hand-forearm mass of $M = 2$ kg must be rejected. These results therefore suggest that the interaction process is closer to inelastic than to elastic, with the effective striking mass being that of the fist alone, as anticipated. Elastic collisions are also ruled out by the high-speed movies, which show that the fist and block are in contact for several milliseconds, and thus appear to stick together.

Although the inelastic collision model is a useful first approximation, it cannot accurately describe the fist-block interaction process. For one thing, it assumes that the collision is completed before the block begins to be deflected, whereas the high-speed movies show that the fist and block are still interacting when fracture occurs. Another shortcoming of the inelastic model is that it gives no insight into the dynamics of the fracture process, nor about the internal

forces acting on the hand-forearm system during the strike.

For a more accurate description of the impact process we used a dynamical model developed by Mishoe and Suggs²⁰ to describe the reaction of the hand to externally imposed vibrations. It is not *a priori* clear that this model, developed to describe the hand's response to vibrating machinery, can be extended to the much larger accelerations developed in a karate strike. Nevertheless, the results are encouraging.

This model (Table III) consists of three masses linked by springs and dampers. The first mass represents the skin, the second (M_1) the nearby hand tissue, and the third (M_2) the remainder of the hand mass (about 90%) and part of the forearm. The first mass is very small compared to the others and may safely be ignored in our application. Thus the hand is described by a pair of coupled linear differential equations of the harmonic oscillator type. The values of the relevant parameters are listed in Table IIIb.

In modeling the strike the hand oscillator system is incident on the block oscillator, described by Eq. (5), with a given initial velocity. Upon contact a system of three coupled oscillators is formed, as in the diagram of Table III. The coupled equations are solved by computer to obtain the deflection of the block as a function of time. In this way curves of maximum deflection as a function of the initial fist velocity are obtained (Fig. 9). The point at which the maximum deflection equals the critical deflection d_0 , then gives the initial fist velocity required for fracture, v_i , from which the corresponding initial energy can be obtained (Table III). The relationship between initial velocity and maximum deflection is linear, and predicts U_i values of 12.3 and 37.1 J for wood and concrete, respectively, somewhat larger than the inelastic values. The corresponding v_i

Table III(b). Parameters used in the dynamic model.

	Mass (kg)	Spring (10^4 N/m)	Damper (N s/m)
Hand	M_1 0.0681	K_1 0.706	B_1 807
	M_2 0.595	K_2 1.16	B_2 275
Block	Wood	k 4.34	
	Concrete	k 295	

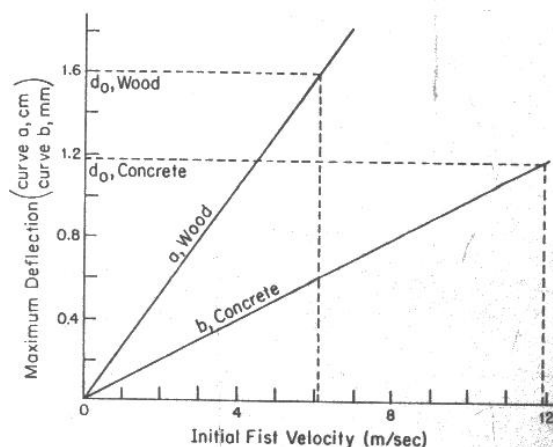


Fig. 9. Maximum deflection of block versus incident fist velocity, predicted by the dynamic model: (a) wood block; (b) concrete block.

values of 6.1 and 10.6 m/s agree with the common observation that beginners can break wooden boards but not concrete patio blocks: First velocities of 6 m/s are within range of a novice, whereas velocities in the 10 m/s range require training and practice.

Many of the details predicted by the dynamic model agree with the empirical data. For example, in the case of concrete the force on the hand rises rapidly, reaching peak values of up to 2200 N, and then falls quickly to zero. The block fractures in less than 5 ms, with peak deflections of about 1 mm. However, the predicted compression of the fist, somewhat under 2 cm, is too large. These predictions do not change greatly when the hand model is simplified by removing the last mass, M_1 , and its associated spring and damper. Eliminating either the remaining spring (K_2) or damper (B_2), however, changes the results considerably and does not lead to reasonable values, even when the remaining spring or damping constant is varied over a wide range. It is interesting to note that in the limiting cases of either large spring constant or large damping constant the predicted value of U_1 approaches the inelastic value. However, this limit is not an accurate description of the actual situation.

These results suggest that with suitable modifications a model of the Mishoe-Suggs type can accurately describe the dynamics of the impact process, and provide useful information regarding the internal forces exerted on the hand and arm during the strike.

VI. BIOMECHANICAL ASPECTS

It is difficult to state a clear-cut criterion for the strength of a hand, foot, or other part of the body employed in a karate strike.²¹ A hand or foot is a complex system of bones connected by visco-elastic tissue. As mentioned earlier, bone is a very strong material, its modulus of rupture being over 40 times larger than that of concrete (Table I). Thus a

cylinder of bone 2 cm in diameter and 6 cm long, simply supported at the ends, can withstand in excess of 25 000 N of force exerted at the center.¹⁵ This value represents a lower limit, since the bones in a striking hand or foot are neither simply supported nor impacted solely at the center. Under impact the bones can move and transmit part of the stress to the muscle and flesh in adjoining areas. Furthermore, some of the impact is absorbed by the skin and the muscles that lie between the point of impact and the bones.²² In addition, much of the local stress is rapidly carried away to other parts of the body.

In the case of the hammerfist strike, for example, the adductor digiti minimi muscle protects the fifth metacarpal, the most vulnerable bone, from the blow. As the fist is tensed the adductor stiffens and thickens. The next line of defense is the set of tendons in the wrist, which cushions the blow as the fist is bent backwards. Finally, the energy transmitted to the arm is absorbed by muscles in the forearm and upper arm.

Proper positioning of the hand or foot is also critical. For example, in many techniques, such as the open hand strike or the side kick, contact is made with the edge of the hand (shuto position) or foot (knife foot). This concentrates the force in a small area of the target and reduces the likelihood of bending a bone to the point of fracture. Thus, if the striking part of the body is correctly oriented, the force required to break it is much greater than that needed to fracture the target.

To illustrate this point, consider breaking a concrete patio block with a side kick, where the foot is in the knifed position [Fig. 10(a)]. Bearing in mind the qualifications discussed above, a rough estimate of the relative strength of the foot as compared to the concrete slab can be made by considering the foot to be a rectangular block of bone of dimensions $l'w'h'$, the side of which strikes the central portion of the flat face of the slab [Fig. 10(b),(c)]. Equation (11) can then be used to compare the forces necessary to frac-

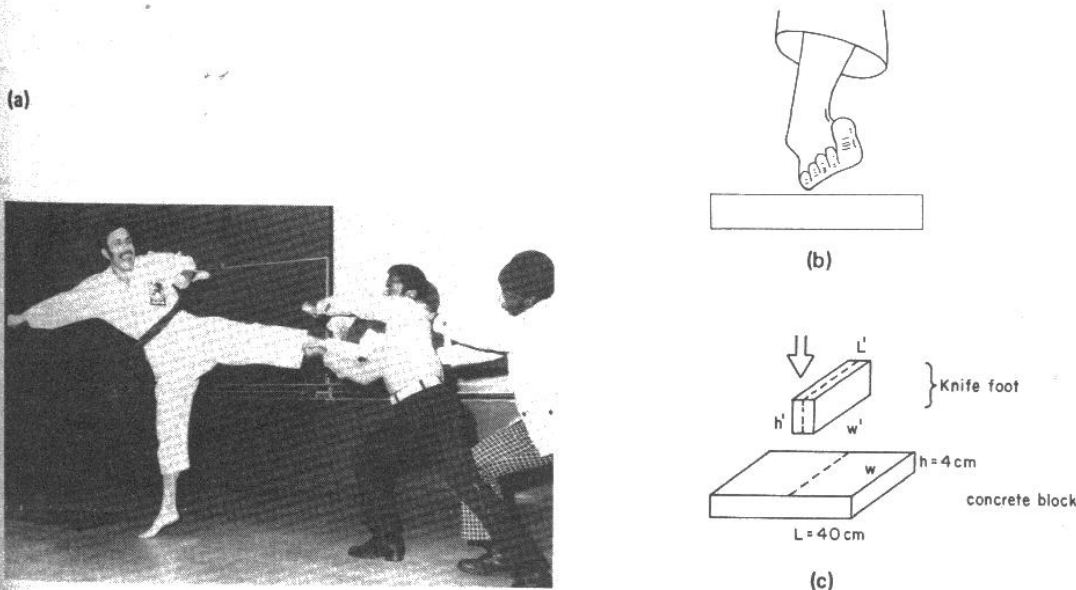


Fig. 10. Importance of orientation in striking a target. (a) Breaking a concrete patio block by means of a side kick. Note the knifed position of the foot. (b) Sketch of relative orientation of foot and block. (c) Model used in calculation. The knifed foot is approximated by a block of bone, oriented as shown.

ture the foot and the slab:

$$\frac{F'_0}{F_0} = \frac{h'^2 w' / l'}{h^2 w / l} \frac{\sigma'_0}{\sigma_0}, \quad (14)$$

where the primed quantities refer to the parameters of the foot. Since the foot is oriented so as to contact the face of the slab with its side surface [Fig. 10(c)], the primed dimensions l', w', h' should be identified as the thickness, length, and width of the foot, respectively. The length and thickness of the foot are comparable to the width and thickness of the concrete, but the width of the foot, typically about 8 cm, is only one-fifth the length of the block ($l = 40$ cm). Accordingly, we shall take $w' = w, l' = h, h' = l/5$. Since $h = 4$ cm, $l/h = 10$. From Table I, $\sigma'_0/\sigma_0 \approx 40$. Accordingly,

$$\frac{F'_0}{F_0} \approx \frac{1}{25} \left(\frac{l}{h}\right)^3 \frac{\sigma'_0}{\sigma_0} \approx 2000. \quad (15)$$

Although this rough estimate is an oversimplification, the general conclusion is valid: A properly positioned foot can withstand forces several orders of magnitude larger than that needed to fracture a concrete slab!

ACKNOWLEDGMENTS

We are indebted to Charlie Miller of the MIT Strobe Lab for his invaluable aid in photographing the strikes, and to Ernie Cravalho, Woodie Flowers, and George Pratt of MIT, and Shelley Simons and Joseph Mansour of Boston's Children's Hospital for useful discussions and loan of equipment. Finally, we thank the members of the St. Paul A.M.E. Karate-Do for their patience and enthusiasm as willing subjects throughout the course of our research. This article is based in part on lecture-demonstrations presented at the 1976 and 1977 annual meetings of the American Association for the Advancement of Science. The authors gratefully acknowledge the encouragement and support of Rolf Sinclair, Secretary of AAAS Section B (Physics), who organized the sessions on "Science for the Naked Eye." This paper is dedicated to the memory of Kanwar Bidhi Chand.

^a Present address: Department of Physics, University of Rochester, Rochester, NY 14627.

^b Present address: NASA—Lyndon B. Johnson Space Center, Houston, TX 77058.

¹ An authoritative treatment is D. F. Draeger and R. W. Smith, *Asian Fighting Arts* (Kodansha International, Palo Alto, CA, 1969).

² J. D. Walker, *Am. J. Phys.* **43**, 845 (1975).

³ H. Blum, *Am. J. Phys.* **45**, 61 (1977).

⁴ P. R. Cavanaugh and J. Landa, *Med. Sci. Sports* **7**, 77 (1975).

⁵ J. A. Vos and R. A. Binkhorst, *Nature* **211**, 89 (1966).

⁶ K. Tuinzing and R. Fischera, *Self-Defense World* (March 1975).

⁷ See, for example, P. M. Morse and K. U. Ingard, *Theoretical Acoustics* (McGraw-Hill, New York, 1968), Sec. 5.1; W. Goldsmith, *Impact: The Theory and Behavior of Colliding Solids* (Edward Arnold, London, 1960), Chap. III; and Ref. 10.

⁸ Note that in the bending process the upper portion of the block is compressed, whereas the lower portion is stretched.

⁹ The following analysis assumes a linear stress-strain relationship up to the point of rupture. Our static loading measurements show that this approximation is valid for wood, but that in concrete it breaks down as σ approaches σ_0 . For concrete we obtained our value of E from the initial slope of the stress-strain curves, and σ_0 from the rupture point. See Ref. 18 for details.

¹⁰ S. C. Crandall, N. C. Dahl, and T. S. Lardner, *An Introduction to the Mechanics of Solids*, 2nd ed. (McGraw-Hill, New York, 1972), pp. 423–24, 514.

¹¹ *Civil Engineering Handbook*, 4th ed., edited by L. C. Urquhart (McGraw-Hill, New York, 1959).

¹² The quasistatic analysis^{2,3} leads to $F_0^q = (8/\pi^2) F_0$ and $U_0^q = (2/3) U_0$. {Blum,³ using a geometrical approximation for the beam deflection [his Eq. (20)] instead of the static loading expression, obtains $U_0^q = (3/2) U_0$.}

¹³ W. Spath, *Impact Testing on Materials* (Gordon and Breach, New York, 1961).

¹⁴ Reference 10, Chaps. 7 and 8. The relationships are more complicated when the force is not applied exactly at $l/2$.

¹⁵ These values were obtained using equations similar to Eqs. (9)–(11) but with $I = \pi a^4/4$, $a =$ radius of cylinder [cf. Eq. (2)], and substituting $y = a$ in Eq. (8) (rather than $h/2$). This gives $d_0 = l^2 \sigma_0 / \pi^2 a E$, $U_0 = (\sigma_0^2 / 16 E) \pi a^2 l$, $F_0 = \pi^3 a^3 \sigma_0 / 4 l$.

¹⁶ See, for example, E. R. Parker, *Materials Data Book* (McGraw-Hill, New York, 1967).

¹⁷ H. Yamada, *Strength of Biological Materials* (Krieger, Huntington, NY, 1970).

¹⁸ S. R. Wilk, "A Biomechanical Study of a Karate Strike," S.B. thesis, MIT, June 1977 (unpublished).

¹⁹ C. E. Clauser, J. T. McConville, and J. W. Young, "Weight, Volume, and Center of Mass of Segments of the Human Body," 1969 AMRL Technical Report, Yellow Springs, OH, Wright-Patterson Air Force Base (unpublished).

²⁰ J. W. Mishoe, "Dynamical Modeling of the Human Hand Using Driving Point Mechanical Impedance Techniques," Ph.D. thesis, North Carolina State University at Raleigh, 1974 (unpublished).

²¹ A detailed discussion of the criteria under which a bone in the body will fracture is given in G. B. Benedek and F. M. H. Villars, *Physics with Illustrative Examples from Medicine and Biology* (Addison-Wesley, Reading, MA, 1974), Vol. 1, Chap. 3.

²² R. M. Alexander, *Animal Mechanics* (University of Washington, Seattle, 1968); Chap. 4.